

Interpretations of Tensile Properties of Polyamide 6 and PET Based Thermoplastics Using ASTM and ISO Procedures

Reference: Jia, N. and Kagan, V. A., “**Interpretations of Tensile Properties of Polyamide 6 and PET Based Thermoplastics Using ASTM and ISO Procedures,**” *Limitations of Test Methods for Plastics, ASTM STP 1369*, J. S. Peraro, Ed., American Society for Testing and Materials, West Conshohocken, PA, 1999.

Abstract: As more and more U.S. companies are looking to convert from ASTM to ISO standards for materials development, testing, and analysis in order to gain greater opportunities and compete more effectively in the global market, it has become increasingly important to deal with the concerns raised during the conversion process, so that the differences can be reconciled and harmonies can be brought into the two sets of standards.

This article presents our investigation on several technical issues in the ASTM and ISO standards on the tensile properties of plastics. Using polyamide (PA) 6 and polyethyleneterephthalate (PET) based thermoplastics as examples, our analysis revealed a range of similarities and differences in these two testing procedures. With either procedure -- ASTM or ISO -- similar results were obtained for material parameters such as tensile strength, tensile strain, and modulus of elasticity, in nonreinforced and short glass fiber reinforced plastics.

The investigation also focused on the role of the system compliance on the tensile strain and modulus measurements, and the effect of grips (wedge- and side-action grips) and gripping on the tensile behavior of the materials. Among the two types of grips, the wedge-action grip was found to cause greater measurement variability, especially in Young's modulus. The analysis of system compliance, on the other hand, reinforced the statements in both testing standards that an accurate strain and modulus measurement would require the use of extensometer. The results in this article went further to indicate how to improve the accuracy in the Young's modulus using the system compliance when the extensometer was not applied during testing. Recommendations were made on the effective use of the testing procedures in product development and design.

Keywords: Polyamide (PA), polyethyleneterephthalate (PET), tensile properties, stress, strain, tensile strength, break, Young's modulus, elasticity, system compliance, grips, ASTM, ISO, design, test

Introduction

In recent years, demands have increased in using polyamide (PA) and polyethyleneterephthalate (PET) products to replace certain metal structures in the automotive vehicle air induction and power train systems, lawn/garden and power tools [1-2]. An average car uses 18 kg of PA and 3 kg of PET. With the annual vehicle production at nearly 12 million, the needed amount of PA is more than 200 million kg and more than 45 million kg for under-the-hood applications alone [3]. The design of these components, especially those critically stressed parts such as vibration welded air intake manifolds [3-4], door and instrument panels, requires advanced analyses of structure [5-6], NVH, welded joints [3], service life [7], and expansion in the envelope of the mechanical behavior to the new level for sophisticated and accurate evaluations of PA and PET.

Concurrent engineering design involving thermoplastic materials relies on information concerning short- and long-term mechanical properties under a wide range of loading and environmental conditions [2] and correct methods of analysis [5] for predicting the mechanical performance of the injection molded parts [8-9].

The influence of time-temperature effects on the tensile strength and tensile-tensile fatigue behavior of short-fiber reinforced polyamides (PA 6 and PA 66) has been reported before [7], and it was found that at room temperature (23°C), the tensile strength of these two thermoplastics are virtually the same. This result has made it possible to simplify our analysis by focusing the compatibility study of tensile properties for one of the two PA plastics mentioned above. The focused tensile property analysis of PA 6 based thermoplastics was presented before [10]. The current paper has extended the scope of that analysis to include other important information from the tensile property testing and analysis.

ISO or ASTM

In the environment of world wide economy, it is increasingly critical for companies with international businesses to have access to reliable and comparable material properties data [6, 11-12] for the product re-design and new product development [13-14]. As the complexity in thermoplastic products is growing, the role of material property testing is gaining importance as well. Today's product designer and toolmaker must consider not only the performance requirements for the injection molded parts, but also the properties of thermoplastics with which the products are made. Certain goals in product design, such as weight reduction, time and cost savings, can only be achieved when considerations in different design areas are combined and optimized [5-6, 13-16].

In this situation, global standardization is playing a more important role than ever in facilitating product manufacturing, marketing, and sales [17]. The widely published testing procedures and specifications for plastic materials by the American Society for Testing and Materials (ASTM, Committee D-20 on Plastics) and the International Standard Organization (ISO) have helped product developers, designers, and molders to establish correct and useful baselines. An important development in the standardization area is the fact that the American automotive industry has become one of the first to

require ISO test procedures for material and product qualifications [18] when the majority testing in the North America is still conducted using ASTM standards. The United States Council for Automotive Research (USCAR) recommended the manufacturers of thermoplastic products to fully convert to ISO test procedures by June 1998.

The decision for this conversion will no doubt have a major impact on material suppliers, molders, designers, and end users when most of the material and product information accumulated for decades and still in use was obtained using ASTM procedures [18]. The current investigation is part of our effort in assisting this transition. The tensile properties of thermoplastics were analyzed not only for the purpose of comparing the ASTM and ISO tensile test procedures, but also because of the importance of tensile properties in the product design.

The current investigation has been focused on the tensile property measurements of PA and PET based thermoplastics. Material parameters obtained using ISO and ASTM specimens and test procedures were compared for their similarities and differences. Analyses were also made on two important aspects of the tensile property measurements, one was the use of extensometer, and another, the effect of grips and gripping on the accuracy of Young's modulus. The purpose of the investigation and analyses is to provide the product designers, product developers, and testing community alike with a guidance in correctly obtaining and interpreting their test results

Materials

The thermoplastics used in this investigation were heat stabilized, unfilled and glass and/or mineral filled polyamide (PA) 6 and polyethyleneterephthalate (PET). Materials were injection molded into ISO multipurpose (ISO 3167:1993 (E)) and ASTM Type 1 and Type 2 (ASTM D 638-97) specimens according to the procedures specified in ISO 294-1, ISO 294-2, ASTM D 3641 and ASTM D 4066. All specimens were sealed (see ASTM D 3892) prior to testing in order to maintain their dry-as-molded (DAM) conditions.

Test Procedures

The tensile property tests were conducted using Instron 4505. Most tests were conducted under standard laboratory conditions (temperature = $23 \pm 2^\circ\text{C}$; relative humidity = $50 \pm 5\%$) on dry-as-molded samples. Some samples were also tested at different temperatures (-40°C and 150°C) using an environmental chamber attached to the Instron. The temperature inside the chamber was controlled at $\pm 2^\circ\text{C}$ within the set point.

Each sample was tested at two crosshead speeds: 1 and 5 mm/min for filled materials, and 1 and 50 mm/min for unfilled materials. The 1 mm/min speed was used to obtain the Young's modulus, while the 5 or 50 mm/min speed was used to obtain other tensile properties such as tensile strength, stresses and strains at yield and break. The tensile strain was measured from the narrow section of each specimen using a clip-on extensometer (ISO 9513 and ASTM E83) with a gage length of 50.8 mm. In some cases the crosshead position was also recorded and used to calculate the apparent strain and

modulus, as discussed later.

The test control and data acquisition were achieved using Instron Series 9 software. The material parameters for tensile properties, such as tensile strength (σ_M), tensile strain at tensile strength (ε_M), stress at break (σ_B) and strain at break (ε_B), were obtained according to the definitions in ASTM D 638 and ISO-527¹. The Young's modulus, E , was calculated according to the definition in ISO-527, which gives

$$E = \frac{\sigma_2 - \sigma_1}{\varepsilon_2 - \varepsilon_1} \quad (1)$$

where $\varepsilon_1 = 0.0005$, $\varepsilon_2 = 0.0025$, and $\sigma_1, \sigma_2 =$ stresses at ε_1 and ε_2 , respectively.

For each sample, a minimum of five specimens were tested under a given condition. The sample mean and sample standard deviation were calculated for each parameter of tensile properties (Table 1).

Results and Discussions

Tensile Properties by ISO and ASTM Standards

In Figures 1 to 3, properties obtained using ISO specimens were plotted against those obtained using ASTM (Type 1) specimens. The solid line, $Y = X$, indicates on the graph where the two sets of property values are equal to each other. For the tensile strength (Figure 1) and strain at tensile strength (Figure 2), the closeness of the data points to this line suggests that the properties obtained using the two standards are practically the same. In fact this was found to be the case for the entire stress-strain relationship [10].

The difference, on the other hand, apparently exists in the Young's modulus where numbers from ISO specimens are often higher than those from ASTM specimens (Figure 3). This difference can be quantified by calculating the ratio between the two sets of modulus numbers using linear regression (Table 2). Ratios were also calculated in the same way for other properties (Table 2). The results indicate that, among the materials in the investigation, the ultimate stresses (σ_M and σ_B) obtained from ISO specimens are on average 2 ~ 3% higher than those from ASTM specimens, and 8% or more can be received from the modulus when test is done on ISO specimens. On the other hand, opposite trend was found in tensile strains where the numbers for ε_M and ε_B are 5 ~ 6% lower in ISO specimens.

Despite the small difference in the nominal cross-sectional areas ($10 \text{ mm} \times 4 \text{ mm} = 40 \text{ mm}^2$ for ISO, $12.7 \text{ mm} \times 3.18 \text{ mm} = 40.4 \text{ mm}^2$ for ASTM Type 1), the different linear dimensions of the two specimens (e.g., the ASTM specimen is wider but thinner than the ISO specimen) might have had an impact on the injection molding process and the distribution of the reinforcement, especially the orientation and distribution of glass fibers. If so, this may be enough to cause a difference in the measured properties. The fact that the deviation in the modulus tends to increase with the amount of glass fibers (Figure 3) further suggests such a possibility.

¹ The definitions of these parameters were considered equivalent in these two standards.

System Compliance and Its Effect on Tensile Strain and Modulus Measurements

Despite the statement in both standards that an extensometer should be used in

Table 1 -- Materials and Their Tensile Properties, 23°C

Material	σ_M , MPa		ϵ_M , %		σ_B , MPa		ϵ_B , %		E , MPa	
	ASTM	ISO	ASTM	ISO	ASTM	ISO	ASTM	ISO	ASTM	ISO
PA 6, 0% G.F. ¹	84.98	87.09	4.24	4.38	—	—	—	—	3140.0	2540.0
<i>St.Dev.</i>	0.66	0.29	0.06	0.10	—	—	—	—	199.2	300.3
PA 6, 15% G.F., 20% M. ¹	117.39	125.01	2.31	2.36	117.37	125.01	2.32	2.36	8846.6	9433.8
<i>St.Dev.</i>	0.32	0.38	0.02	0.04	0.33	0.38	0.04	0.04	136.2	247.1
PA 6, 15% G.F., 20% M. – 40°C	163.77	169.70	2.78	2.90	163.77	169.70	2.78	2.90	10578.6	9732.0
<i>St.Dev.</i>	1.92	2.23	0.04	0.10	1.92	2.23	0.04	0.10	204.2	956.4
PA 6, 15% G.F., 20% M. 150°C	45.60	47.59	8.39	7.90	45.32	47.39	8.79	8.40	3227.1	2869.0
<i>St.Dev.</i>	0.44	0.37	0.20	0.30	0.40	0.36	0.29	0.50	119.8	214.5
PA 6, 30% G.F., Recycled	150.11	166.30	2.20	2.29	149.21	166.14	2.33	2.32	10522.7	11826.9
<i>St.Dev.</i>	0.34	0.23	0.04	0.04	0.61	0.40	0.07	0.07	436.2	331.1
PA 6, 33% G.F.	176.66	180.70	2.83	2.86	175.62	179.90	3.02	3.00	9788.8	10410.0
<i>St.Dev.</i>	1.14	1.02	0.05	0.11	1.00	1.19	0.07	0.25	493.0	1666.4
PA 6, 33% G.F., I.M. ¹	143.59	151.71	2.60	2.67	142.50	149.75	2.79	2.89	9372.0	9431.6
<i>St.Dev.</i>	0.27	0.70	0.04	0.01	0.36	0.81	0.06	0.07	297.4	689.6
PA 6, 40% M. & G.F.	119.17	129.09	2.31	2.30	119.15	129.09	2.32	2.31	10584.3	12430.7
<i>St.Dev.</i>	0.90	0.45	0.02	0.05	0.91	0.45	0.04	0.06	333.6	801.2
PA 6, 50% G.F.	212.58	220.84	2.62	2.51	212.46	220.76	2.66	2.54	14890.0	18700.0
<i>St.Dev.</i>	1.09	2.46	0.07	0.14	1.33	2.46	0.10	0.15	1085.9	3464.6
PET, 30% G.F.	156.78	153.09	2.57	2.43	156.78	153.03	2.58	2.45	11586.3	10786.9
<i>St.Dev.</i>	0.98	0.29	0.03	0.04	0.98	0.37	0.04	0.07	156.2	507.7
PET, 35% M. & G.F.	127.66	126.45	1.73	1.57	127.66	126.45	1.73	1.57	12570.5	12417.8
<i>St.Dev.</i>	1.06	1.62	0.05	0.09	1.06	1.62	0.05	0.09	213.5	601.9

¹ G.F., M., I.M.: glass fiber reinforced, mineral reinforced, and impact modified, respectively.

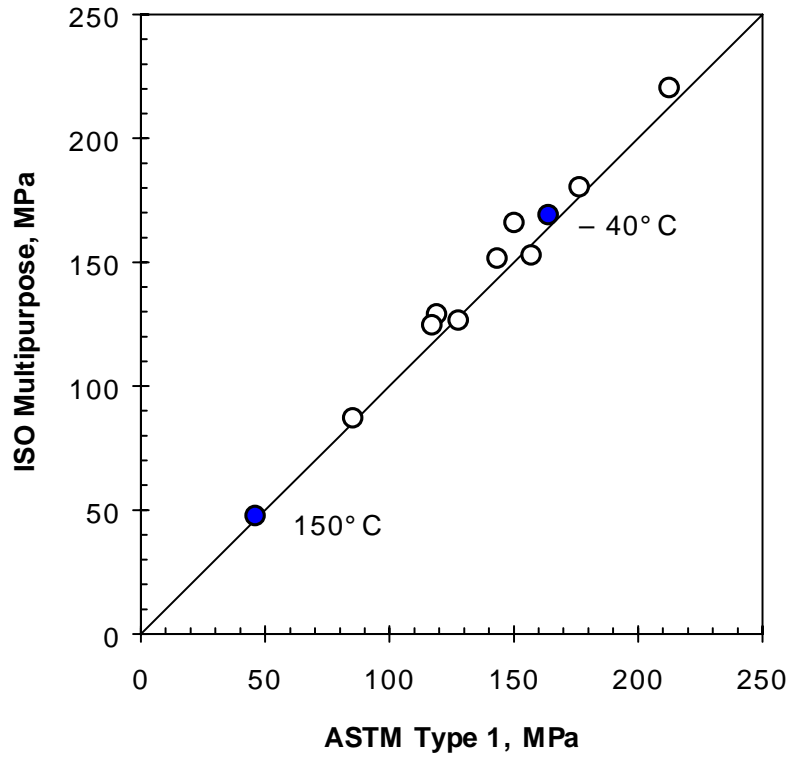


Figure 1 -- Tensile Strength of Materials, σ_M . $T = 23^\circ\text{C}$ unless otherwise indicated.

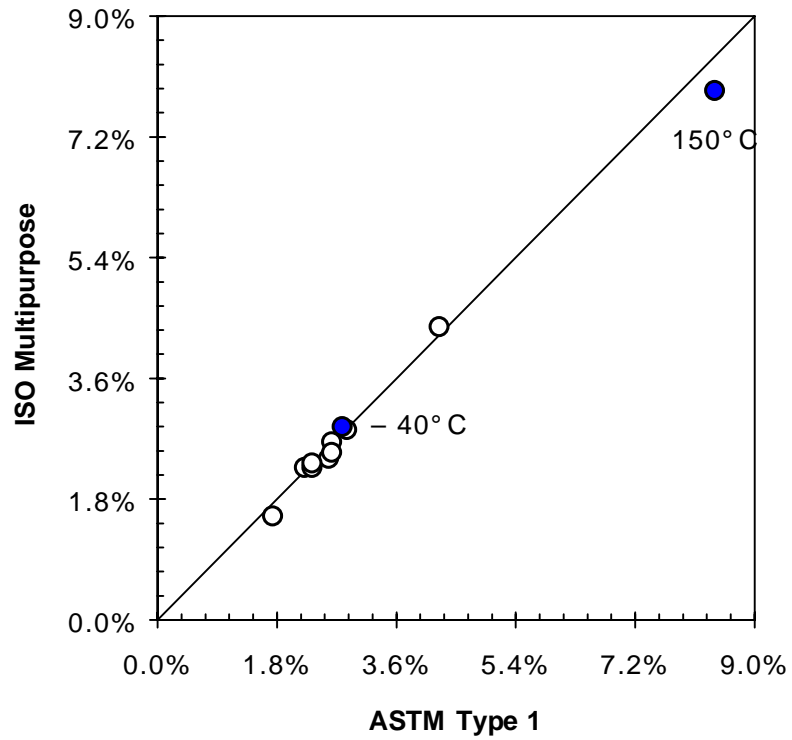


Figure 2 -- Tensile Strain at Tensile Strength, ϵ_M . $T = 23^\circ\text{C}$ unless otherwise indicated.

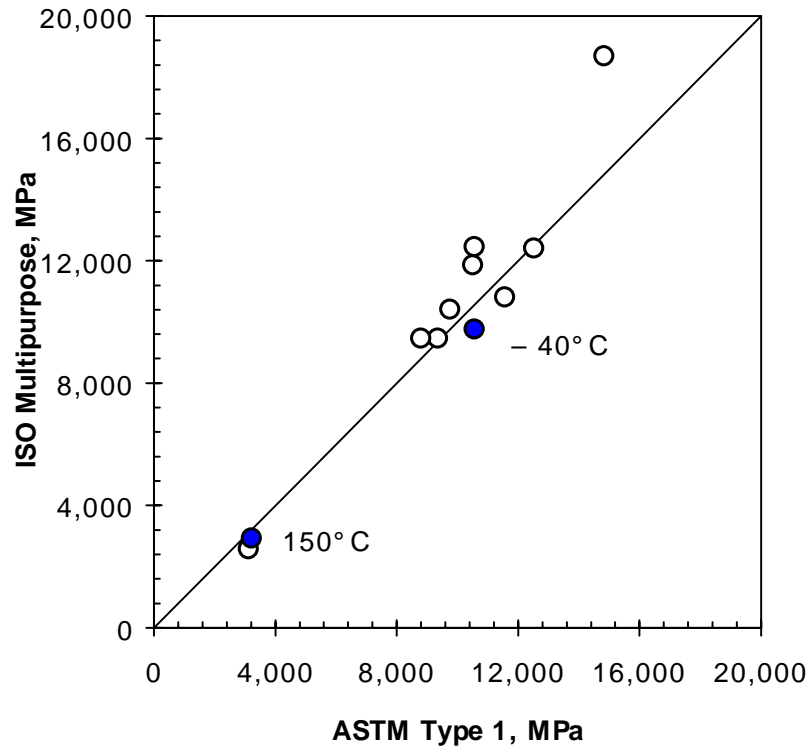


Figure 3 -- Young's Modulus, E . $T = 23^{\circ}\text{C}$ unless otherwise indicated.

Table 2 -- Ratios between ISO and ASTM Property Parameters

	σ_M	ϵ_M	σ_B	ϵ_B	E^1
ISO \div ASTM ²	1.028 \pm 0.04	0.934 \pm 0.024	1.022 \pm 0.039	0.947 \pm 0.019	1.082 \pm 0.126
r^2 (coef. corr.)	0.987	0.994	0.984	0.997	0.924

¹ The modulus value for PA 6, 50% G.F. was not used in calculating this ratio.

² ISO \div ASTM = (slope in regression) \pm 1 (standard error).

elongation measurement, use of such device may not always be possible or convenient. At low temperature (e.g., -40°C), certain mechanisms in the extensometer tend to be frozen and the surface of the specimen can be slippery, making the extensometer difficult to attach or operate. At high temperature, handling of the extensometer may also be proven to be difficult for the lab operator, especially when limited to the tight space in the chamber [20]. Without extensometer, however, one must find alternatives with which the elongation, strain, and modulus can be calculated. The purpose of this section is to analyze such an alternative and estimate the errors associated with the measurement method.

Next to the use of extensometer, the obvious way of obtaining tensile strain is to calculate the change in so-called grip to grip distance, ΔL , as shown in Figure 4. In

reality, however, ΔL rarely gets measured directly; instead it is the change in the crosshead position, ΔX , that is recorded and used in the strain calculation. For the purpose of the current discussion, the strain based on ΔX is called apparent strain, which is defined as $\varepsilon_a = \Delta X/L$. The apparent modulus, on the other hand, can be defined as

$$E_a = \frac{\sigma_{a2} - \sigma_{a1}}{\varepsilon_{a2} - \varepsilon_{a1}} \quad (2)$$

where $\varepsilon_{a1} = 0.0005$, $\varepsilon_{a2} = 0.0025$, and σ_{a1} and σ_{a2} are stresses at ε_{a1} and ε_{a2} , respectively.

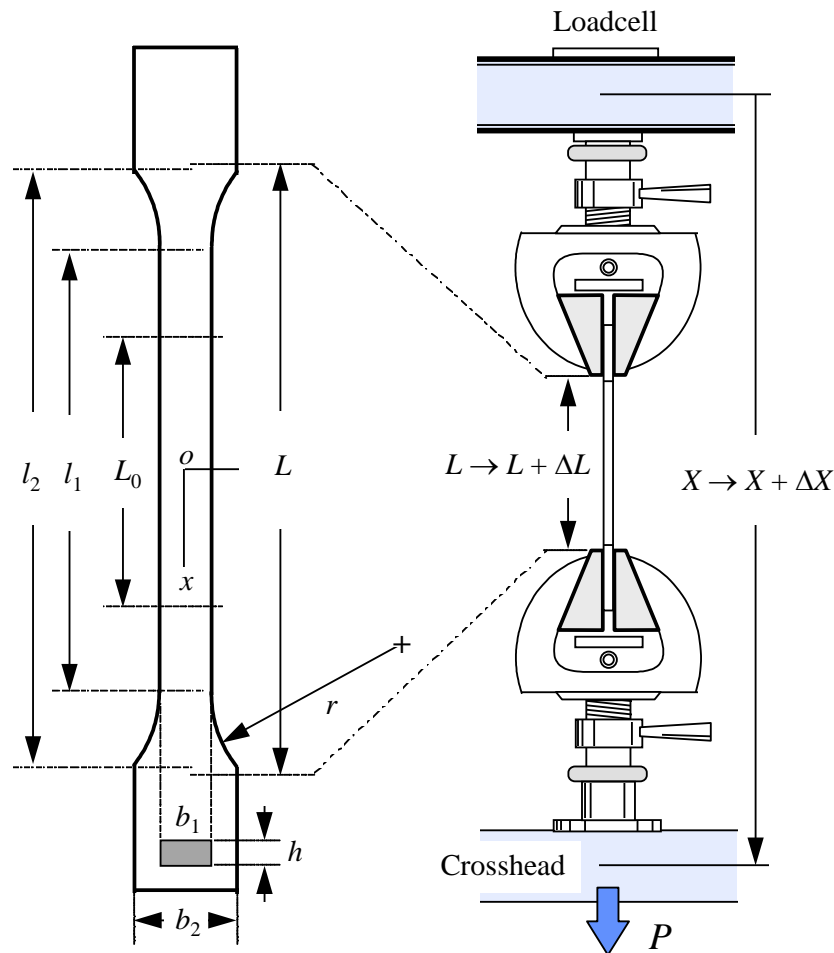


Figure 4 -- Tensile Specimen and Test Setup (ISO 527-2:1993(E); Table 4).

To substitute ε and E with ε_a and E_a , one may encounter errors in two ways: (1) Unlike in the section defined by the gage length L_0 , the stress and strain in L is not always simple and uniaxial, especially at the vicinity of the grips where complex stress and strain distribution is expected; (2) Use of ΔX will include the deformation of the testing machine in the strain calculation, making the results machine dependent, therefore less reliable and less reproducible.

To quantify the above analysis, notice first that the ΔX can be expressed as

$$\Delta X = \Delta S + \Delta L \quad (3)$$

where ΔS is the total machine deformation which may include deformation from the loadcell, the crosshead beam, and the grips and connectors. Assume further that the stress and strain are uniform across any cross-section in L , and the contributions by other stress components to the specimen elongation are negligible. In this case one may have

$$\Delta L = 2 \int_0^{L/2} \varepsilon(x) dx = 2 \int_0^{L/2} \frac{\sigma(x)}{E} dx = \frac{2P}{Eh} \int_0^{L/2} \frac{dx}{b(x)} \quad (4a)$$

or

$$\Delta L = m \cdot \Delta L_0 \quad (4b)$$

where P = applied load, $b = b(x)$ ($b_1 \leq b(x) \leq b_2$) and h = constant are the width and thickness of the specimen, ΔL_0 is the change in gage length. The ratio between ΔL and ΔL_0 is expressed by a deformation parameter m ,

$$m = \frac{1}{L_0} \left\{ l_1 + \frac{b_1}{b_2} (L - l_2) + b_1 \left[\frac{1 + 2r/b_1}{\sqrt{1 + 4r/b_1}} \cos^{-1} \sqrt{\frac{b_1}{b_2} \left(1 - \frac{b_2 - b_1}{4r} \right)} - \frac{1}{2} \cos^{-1} \left(1 - \frac{b_2 - b_1}{2r} \right) \right] \right\} \quad (5)$$

The definitions of parameters in Eq.(5), b_1 , b_2 , l_1 , l_2 , and r , are consistent with those given in ISO 527-2:1993(E) (Figure 4). To derive Eq.(5) it was also assumed that ΔL and ΔL_0 are both proportional to the applied load, i.e. the material is essentially elastic. The analysis below is therefore restricted in the region where the stress and strain are linearly related². The numerical values for m for different types of tensile specimens are shown in Table 3.

Furthermore, assume that the overall deformation of the machine, ΔS , is proportional to P , Eq.(3) can then be written as

$$\Delta X = s \cdot P + m \cdot \Delta L_0 \quad (6)$$

where s is defined as system compliance.

With the help of Eq.(6), the apparent strain can be expressed in terms of the “real strain” ε as

² It is possible to extend the current analysis to the entire stress-strain region by replacing $\varepsilon = \sigma/E$ in Eq.(4a) with a more general relationship $\varepsilon = \varepsilon(\sigma)$ that can be established experimentally. The consequence, however, is that one must deal with a parameter m that is likely to be stress dependent, and the overall calculation may no longer be simple enough to make the effort practical.

$$\varepsilon_a = \frac{s \cdot P + m \cdot \Delta L_0}{L} = \left(\frac{s \cdot A}{L} \right) \sigma + m \cdot \left(\frac{L_0}{L} \right) \varepsilon \quad (7)$$

where $A = b_1 \cdot h =$ initial cross-sectional area.

Using Eq.(7), the change in ε_a can be related to changes in σ and ε , i.e., $\Delta\varepsilon_a = (s \cdot A / L)\Delta\sigma + m \cdot (L_0 / L)\Delta\varepsilon$. This relationship can be applied to express the apparent Young's modulus in terms of the "real modulus" E :

$$E_a = \frac{\Delta\sigma}{\Delta\varepsilon_a} = \frac{\Delta\sigma}{\Delta\varepsilon} \div \frac{\Delta\varepsilon_a}{\Delta\varepsilon} = \frac{E}{(s \cdot A / L)E + m \cdot (L_0 / L)} \quad (8)$$

where the assumption is made for $\Delta\sigma / \Delta\varepsilon = (\sigma_2 - \sigma_1) / (\varepsilon_2 - \varepsilon_1) = E$. In situations where E_a , rather than E , is obtained, Eq.(8) can be rearranged to give an estimate on E once the system compliance s is known. In this case, one has that

$$E' = \frac{m(L_0 / L)E_a}{1 - (s \cdot A / L)E_a} = \frac{(m \cdot L_0)E_a}{L - (s \cdot A)E_a} \quad (9)$$

In this equation, the symbol E' has been used in order to differentiate its value from the original E obtained in Eq.(1).

Table 3 -- Parameter m for ISO and ASTM Specimens¹

Type of Specimen	m	L_0 (mm)	L (mm)	l_1 (mm)	l_2 (mm)	b_1 (mm)	b_2 (mm)	r (mm)
ISO	1.60	50.8	115	59.0	115	9.86	19.7	82
ASTM Type 1	1.72	50.8	115	60.8	102	12.56	18.9	68
ASTM Type 2	1.68	50.8	135	60.3	118	6.23	19.0	68

¹ The geometric parameters used in calculating m can be found in ISO 527-2:1993(E) and in Figure 4.

To see how the above analysis can be applied, one may follow the steps outlined below:

- (1) Obtain the numeric data for ΔX_i , ΔL_{0i} , and P_i , where $i = 1, 2, \dots, n$, and n is the total sampling points;
- (2) Calculate a new data series, $\Delta X_i - m \cdot \Delta L_{0i} = (\Delta X - m \cdot \Delta L_0)_i$, where m is obtained from Table 3 according to the type of the specimen (ISO or ASTM);
- (3) Run a linear regression on P_i and $(\Delta X - m \cdot \Delta L_0)_i$ in a region roughly defined by $0.0005L < \Delta X_i < 0.025L$, or $0.0005 < \varepsilon_a < 0.0025$;
- (4) Use the slope calculated in step (3) as the system compliance, s ;
- (5) Calculate E and E_a from Eqs.(1) and (2), and calculate E' from Eq.(9) using s and E_a .

The calculated system compliance s , is shown in Table 4 for a number of samples. Interestingly enough, the number s was found to be actually dependent on modulus E_a or

E , as demonstrated clearly in Figure 5. An empirical relationship can be easily found to be

$$s = 86.592 \times E_a^{-0.6269} . \quad (10)$$

Using Eq.(10), the system compliance for each material sample was recalculated and the results (s^*) can be found in Table 4 for a direct comparison with s .

Table 4 -- Calculation of System Compliance

Material and Specimen Type	s (mm/kN)	$s^* =^1$ $86.592 \times E_a^{-0.6269}$
PA 6, 0% -- ASTM Type 1	0.739	0.738
PA 6, 14% G.F., I.M. -- ISO	0.616	0.595
Same as above, 120°C	0.850	0.866
PA 6, 33% G.F., I.M. -- ASTM	0.477	0.479
PA 6, 40% G.F. -- ISO	0.383	0.390
PET, 45% G.F. -- ISO	0.383	0.382

¹ The numeric values for E_a can be found in Table 5.

The dependence of s on E_a or E raised an interesting question concerning the nature of the system compliance which was thought originally to reflect only the deformation of the testing machine, not the material properties. By measuring directly the grip separation during the course of elongation rather than relying on the return of the crosshead position ΔX , we found that most of the machine deformation, $(\Delta X - m \cdot \Delta L_0)$, actually occurred within the area where the specimen was clamped. It was believed that the portion of the specimen between the gripping faces contributed significantly to the overall deformation ΔX . Little surprise then that the quantity represented by $(\Delta X - m \cdot \Delta L_0)$, and eventually s , would be material property dependent since the grip-to-grip elongation, $\Delta L = m \cdot \Delta L_0$, did not take into account the deformation of the specimen between the gripping faces.

An important implication from Eq.(10) is that one may obtain the correction for E_a (i.e., E') even if the system compliance cannot be obtained from the materials to be tested. To do so, one needs to obtain at first the numerical expression in Eq.(10) by testing several controlled materials with known stress-strain relationships that allow s to be derived from steps (1) ~ (5) stated above. Once s is known and s - E_a relationship is established, E' can be calculated using Eq.(9) for any material sample with E_a obtained experimentally. E' represents the correction to E_a , which is expected to give a modulus value much closer to E without using an extensometer. The step-by-step procedure to obtain E' from s and E_a is summarized as follows:

(A) Test controlled samples without extensometer, and obtain P_i , ΔX_i , and $(\Delta X - m \cdot \Delta L_0)_i$, where ΔL_{0i} can be calculated from the known stress-strain relationship;

(B) Follow steps (3) to (5) above to calculate the apparent modulus E_a and the system compliance s ;

(C) Plot s against E_a , and establish the empirical relationship such as the one shown in Eq.(10)³;

(D) Test new samples using the same setup, and calculate E_a ;

(E) Calculate E' from Eq.(9), using s obtained from Eq.(10).

A few examples of such calculations have been given in Table 5. The effectiveness of the above procedures can be seen clearly from the calculated errors $\Delta(E_a, E) = (E_a - E) / E \times 100$, and $\Delta(E', E) = (E' - E) / E \times 100$.

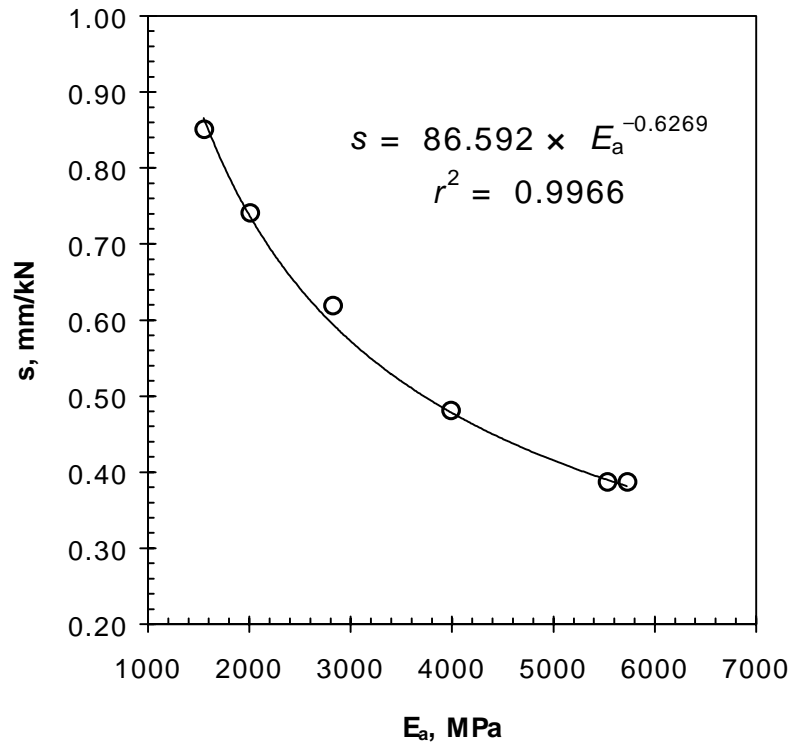


Figure 5 -- System Compliance vs. Apparent Young's Modulus (Table 4). $r^2 =$ coefficient of correlation.

The Effect of Grips and Gripping on Modulus Measurement

One of the observations from the tensile test was that although the sample standard deviation for stress (e.g., σ_M and σ_B) is normally very small, the same deviation is greater for strain, and greater still for Young's modulus. Using the coefficient of variation (CV) to characterize the data scattering, where $CV = (\text{sample standard deviation}) \div (\text{sample mean})$, it was found that CV is 0.2 ~ 1.5% for stress, 2 ~ 5% for strain, and 2 ~ 10% for modulus.

In order to understand the progressive increase in CV from stress to strain, and from strain to modulus, a closer examination was made on the stress-strain relationship

³ Since the relationship in Eq.(10) is purely empirical, one should be able to choose any mathematical expression deemed to best fit the data at hand.

between $\varepsilon = 0$ and 0.3% where the modulus was calculated. It was found that in many cases the behavior of the stress-strain curve was rather complicated initially around $\varepsilon = 0$ (Figure 5). The CV for the modulus could increase significantly when this initial region extended beyond $\varepsilon = 0.05\%$. This situation was found to be worse in some samples than in others.

Table 5 -- Correction of Young's Modulus Using System Compliance

Material and Specimen Type	s^* (mm/kN)	E_a (MPa)	E (MPa)	E'^1 (MPa)	$\Delta(E_a, E)^2$	$\Delta(E', E)^2$
PA 6, 0% G.F. -- ASTM ³	0.789	1798.5	2658.6	2729.2	-32.4%	2.65%
PA 6, 14% G.F., I.M. -- ISO ³	0.595	2821.2	4685.7	4628.8	-39.8%	-1.21%
Same as above, 120°C	0.849	1598.6	1918.3	2092.1	-16.7%	9.06%
PA 6, 14% G.F., I.M. -- ASTM	0.487	3878.2	9606.7	8797.8	-59.6%	-8.42%
Same as above, ASTM Type 2	0.328	7280.6	9813.3	9244.4	-25.8%	-5.80%
PA 6, 40% G.F. -- ISO	0.390	5531.0	13137.7	14621.8	-57.9%	11.3%
PET, 45% G.F., -- ISO	0.382	5724.0	15833.5	15687.8	-63.9%	-0.92%
PET, 15% G.F., -- ISO, 150°C	0.977	1278.9	1918.3	1566.4	-33.3%	-18.3%

¹ The corrected Young's modulus based on Eq.(9).

² $\Delta(E_a, E) = (E_a - E) / E \times 100$; $\Delta(E', E) = (E' - E) / E \times 100$.

³ ASTM Type 1 and ISO multipurpose specimens, respectively (see Table 3).

To find out why this was the case, the specimen elongation and the applied force were compared from one sample point to the next, as shown in Figure 6. It was noticed that, at the beginning of the tensile test, the applied force does not always increase as the position of the crosshead changes. Instead the force remains unchanged or even decreases following an initial increase. After a while it increases again and this time the change is more rapid. Corresponding to the force, the elongation measured by the extensometer also exhibits a strange pattern in the same region.

An explanation for this phenomenon can be given knowing that the force has been transferred to the specimen through a pair of wedge action, or self-tightening, grips. The decrease in force following an initial increase can be considered to be a result of the grips biting into the material (Figure 7). The indentation by the serrated grip faces may have caused certain plastic flow on the surface of the specimen, and it apparently has been sensed by the extensometer as suggested by the elongation behavior seen in Figure 7. The combination of the surface indentation and the surface plastic flow appears to be what gave the erroneous stress-strain behavior that in turn caused large variations in strain and modulus.

To verify this hypothesis, tensile tests were conducted on a few samples using a pair of side-action grips in which the on-going surface indentation is not an issue due to the lack of self-tightening. Figure 8 shows the stress-strain in the same region as Figure 7. Sure enough, the force and elongation behavior that caused large errors is no longer there. The significantly reduced variability is obvious in Figure 5 where the stress-strain

curves with wedge-action and side-action grips are compared. The comparison between the CV's from samples using two types of grips is given in Table 6.

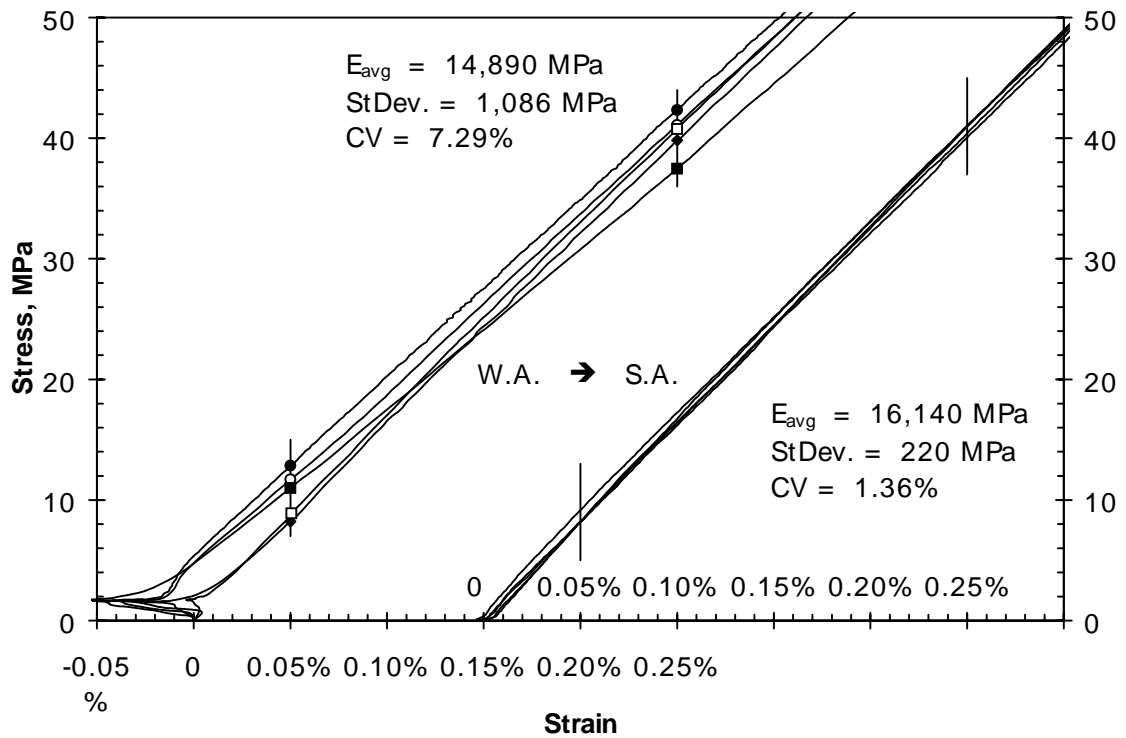


Figure 6 -- *Effect of Grips on the Tensile Behavior of Thermoplastics (PA 6, 50% G.F.). The variation in modulus measurement associated with the wedge-action grips (W.A.) is seen to be reduced significantly with the use of side-action grips (S.A.).*

The problem with using the side-action grips is that specimens with high tensile strength often slip between the grips in the mid of testing. This problem, however, should not affect the modulus measurement since the slipping usually occurs far after $\epsilon = 0.0025$.

Conclusions

(1) Tensile strength and deformation parameters of PA 6 and PET obtained by ISO and ASTM methods are generally compatible; both can be used for the design of injection molded, non-reinforced and glass fiber reinforced parts and the material pre-selection.

(2) For the structural design of the critically stressed plastic components, design optimization for mechanical performance, weight reduction, and so on, it is very important to ensure that the accurate ISO or ASTM tensile property data is utilized.

(3) The ISO tensile test data for stress and modulus is found to be slightly higher than that of ASTM for reinforced and non-reinforced semicrystalline PA 6, PET, and amorphous PP [18].

(4) The value of Young's modulus can be significantly affected by the method of tensile strain calculation, which can be obtained with or without an extensometer.

(5) Use of wedge-action grips may cause large variability in strain and modulus calculation, and this variability can be reduced significantly by using the side-action grips.

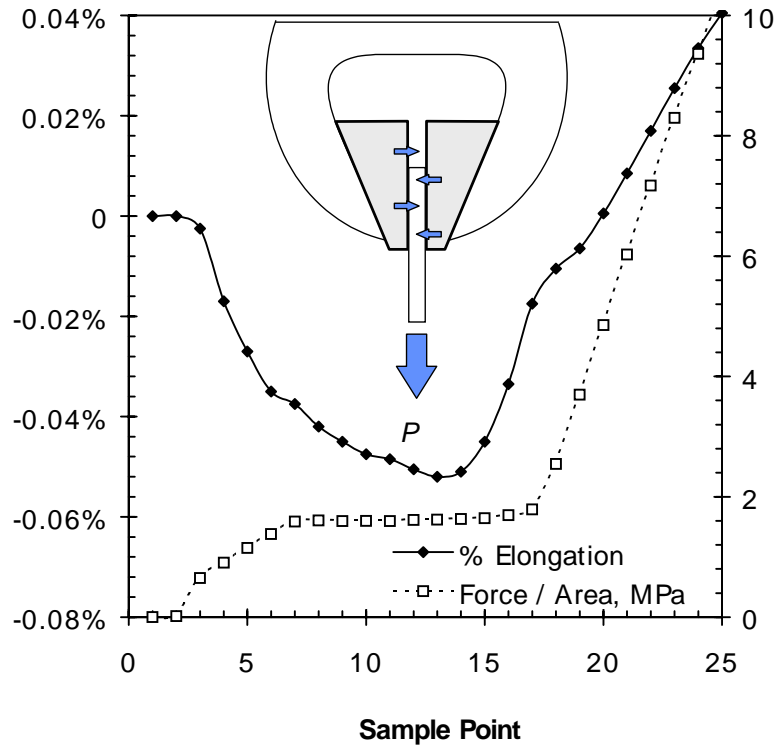


Figure 7 -- *The Self-Tightening of the Wedge-Action Grips Was Considered to be Responsible for the Large Variability in Strain and Modulus Measurement (Figure 5).*

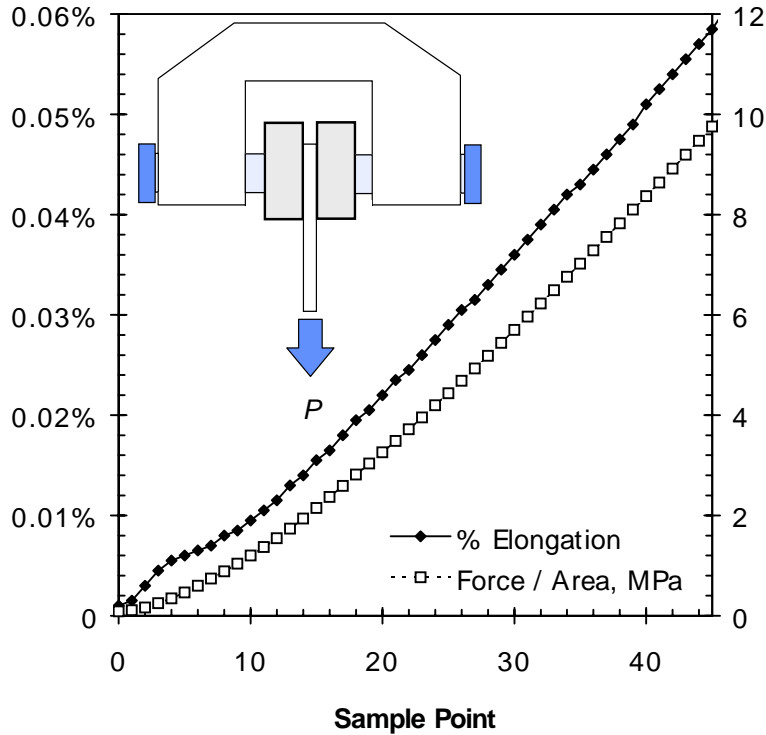


Figure 8 -- “Well-Behaved” Stress and Strain Curves with the Use of Side-Action Grips.

(6) The suggested tensile strains for calculating Young’s modulus (ISO 527-1:1993(E)), $(\varepsilon_2 - \varepsilon_1) = (0.0025 - 0.0005)$, are not the best to satisfy the needs for an accurate modulus value. Practically it will be more convenient to use $\varepsilon_2 = 0.005$.

Table 6 -- Coefficient of Variation for Young’s Modulus and the Effect of Grips on Measurement Variability

Material and Specimen Type	Grips	E (MPa)	St.Dev. (MPa)	CV
PET, 30% G.F. -- ISO ¹	W.A. ²	12,101	996.4	8.23%
	S.A. ²	12,592	166.1	1.32%
PA 6, 0% G.F. -- ASTM ¹	W.A.	3,140	199.2	6.34%
	S.A.	3,150	109.4	3.47%
PA 6, 0% G.F. -- ISO	W.A.	2,540	300.3	11.82%
	S.A.	2,850	117.8	4.13%
PA 6, 12% G.F. -- ISO	W.A.	6,292	705.5	11.21%
	S.A.	5,805	107.5	1.85%
PA 6, 33% G.F. -- ASTM	W.A.	9,790	493.0	5.04%
	S.A.	10,600	370.0	3.49%
PA 6, 33% G.F. -- ISO	W.A.	10,410	1,666.0	16.01%
	S.A.	9,630	360.4	3.74%
PA 6, 50% G.F. -- ASTM	W.A.	14,890	1,086.0	7.29%

	S.A.	16,140	220.0	1.36%
PA 6, 50% G.F. -- ISO	W.A.	18,700	3,465.0	18.53%
	S.A.	16,100	668.0	4.15%

¹ ISO multipurpose and ASTM Type 1 specimens, respectively.

² W.A. -- wedge-action grips; S.A. -- side-action grips.

References

- [1] "Composites Makes Progress Under the Bonnet", *Reinforced Plastics*, May 1997, pp. 28-32.
- [2] Roast, D. and Di Mattia, D., *Designing with Plastics and Composites: A Handbook*, Van Nostrand Reinhold, New York, 1993, 979 pages.
- [3] Carlson, E., Nelson, K., "Nylon Under-the-Hood: A History of Innovation", *Automotive Engineering*, December, 1996, pp. 84-89.
- [4] Kagan, V., "Vibration Welding of Glass Fiber Reinforced Polyamide Plastics", *Kunststoffe, European plastics*, December, 1997, pp. 1804-1807.
- [5] Trantina, G. and Nimmer, R., *Structural Analysis of Thermoplastic Components*, McGraw-Hill, Inc., 1994, 366 pages.
- [6] Beiter, A., Cardinal, J. M., and Ishii, K., "Preliminary Plastic Part Design: Focus on Material Selection and Basic Geometry While Balancing Mechanical Performance and Manufacturing Cost", *Journal of Reinforced Plastics and Composites*, Vol. 16, No. 14/97, pp. 1293-1302.
- [7] Jia, N. and Kagan, V. A. "Effects of Time and Temperature conditions on the Tensile-Tensile Behavior of Short Fiber Reinforced Polyamides", *ANTEC'97, SPE Conference Proceedings*, Vol. 2, pp. 1844-1848.
- [8] Kwok, W. and Choy, C. L., "Elastic Moduli of Injection-Molded Short-Glass-Fiber-Reinforced Poly (ethylene terephthalate)", *Journal of Reinforced Plastics and Composites*, Vol. 16, No. 4/1997, pp. 290-305.
- [9] *Engineering Plastics*, Engineering Materials Handbook, Vol.2, ASM International, 1988, 883 pages.
- [10] Jia, N. and Kagan, V. A., "Compatibility Analysis of Tensile Properties of Polyamides Using ASTM and ISO Testing Procedures", *SPE Conference Proceedings*, ANTEC'98, Vol.2, Materials, pp. 1706-1712.
- [11] Reinnertsen, C., "Testing Requires a Delicate Balance", *Machine Design*, May 28, 1993, pp. 62-71.
- [12] "Testing, Testing", *Reinforced Plastics*, June 1993, pp. 48-52.

- [13] Oehler, R., Graichen, C., and Trantina, G., “Design-Based Material Selection”, *Plastics Engineering*, January 1995, pp. 25-28.
- [14] Wigodsky, V., “Plastics Testing”, *Plastics Engineering*, October 1997, pp. 22-26.
- [15] Rackowitz, R., “Looking Beyond the Materials Data Sheet”, *Plastics Design Forum*, May 1994, pp. 28-31.
- [16] Wigodsky, V., “The Road to Standardization”, *Plastics Engineering*, April 1995, pp. 22-28.
- [17] Gabriele, C., “Global Standards Could Resolve Inconsistencies”, *Plastics Technology*, June 1993, pp. 48-55.
- [18] *Uniform Global Testing Standards: A Technical Primer*, The Society of the Plastics Industry, Inc., 1996, 52 pages.
- [19] Verne, L. “Comparable Data for Plastic Materials -- Help is on the Way”, *Plastics Design Forum*, January-February 1993, pp. 37-40.
- [20] Turek, E., “On the Tensile Testing of High Modulus Polymers and the Compliance Correction”, *Polymers Engineering Science*, Vol.33, 1993, pp. 328-333.

This information is provided for your guidance only. We urge you to make all tests you deem appropriate prior to use. No warranties, either expressed or implied, including warranties of merchantability or fitness for a particular purpose, are made regarding products described or information set forth, or that such products or information may be used without infringing patents of others.

BASF Corporation
3000 Continental Drive - North
Mount Olive, New Jersey 07828-1234

www.basf.com/usa
www.plasticsportal.com

©Copyright BASF Corporation 2003

HELPING MAKE PRODUCTS BETTER™

BASF